ApJ, in press
Preprint typeset using LaTeX style emulateapj v. 03/07/07



# SECULAR ORBITAL DYNAMICS OF HIERARCHICAL TWO PLANET SYSTEMS

Dimitri Veras[1], Eric B. Ford[1]

*ApJ, in press*

## ABSTRACT

The discovery of multi-planet extrasolar systems has kindled interest in using their orbital evolution as a probe of planet formation. Accurate descriptions of planetary orbits identify systems which could hide additional planets or be in a special dynamical state, and inform targeted follow-up observations. We combine published radial velocity data with Markov Chain Monte Carlo analyses in order to obtain an *ensemble* of masses, semimajor axes, eccentricities and orbital angles for each of 5 dynamically active multi-planet systems: HD 11964, HD 38529, HD 108874, HD 168443, and HD 190360. We dynamically evolve these systems using 52,000 long-term N-body integrations that sample the full range of possible line-of-sight and relative inclinations, and we report on the system stability, secular evolution and the extent of the resonant interactions. We find that planetary orbits in hierarchical systems exhibit complex dynamics and can become highly eccentric and maybe significantly inclined. Additionally we incorporate the effects of general relativity in the long-term simulations and demonstrate that can qualitatively affect the dynamics of some systems with high relative inclinations. The simulations quantify the likelihood of different dynamical regimes for each system and highlight the dangers of restricting simulation phase space to a single set of initial conditions or coplanar orbits.

*Subject headings:* celestial mechanics — planetary systems: formation — methods: N-body simulations, statistical

## 1. INTRODUCTION

Currently, over 30 multi-planet exosystems are each known to include 2-5 known planets. The orbital architectures and formation scenarios for these systems have become subjects of numerous investigations. The recent discovery of a fifth planet around 55 Cnc (Fischer et al. 2008) has prompted a flurry of follow-up studies (Gayon et al. 2008; Raymond et al. 2008a; Ji et al. 2009) that aim to better describe the dynamics and evolution of that system. Despite sparse data, the directly-imaged triple system HR 8799 (Marois et al. 2008) has been subject to intense scrutiny (Fabrycky & Murray-Clay 2008; Close & Males 2009; Fukagawa et al. 2009; Goździewski & Migaszewski 2009; Lafrenière et al. 2009; Reidemeister et al. 2009; Sudol et al. 2009). These explorations demonstrate that major open questions regarding multi-planet systems remain, including: What is the timescale for instability in these systems? Could they admit additional, currently undetectable planets? How tightly "packed" are such systems (e.g. Raymond et al. 2009)?

These questions can be addressed by investigating the orbital evolution of individual planetary systems. How do the orbital eccentricities and semimajor axes of planets change with time? How does additional physics (e.g. tidal forces and general relativity, henceforth referred to as GR) affect the orbits of short-period planets and indirectly other planets in the system? Theoretical investigations addressing these questions should account for the uncertainties in orbital parameters obtained from observations. In order to study dynamics, we need to establish initial conditions. Unfortunately, the accuracy of such initial conditions are limited due to measurement uncertainties and degeneracies inherent to the radial velocity (RV) exoplanet discovery technique. Occasionally, the best-fit RV data yields parameters which indicate that the timescale for such a system to undergo instability is much less than the age of the system (e.g., in less than $10^5$ yr, for HD 82943; Mayor et al. 2004; Fabrycky & Murray-Clay 2008). These short timescales (relative to system lifetimes) suggest that the best-fit orbital model is unlikely and motivate investigations to find the plausible and stable solutions. Further, both $i_{rel}$ and $i_{LOS}$ for planets in most multi-planet systems have not yet been measured. Noteworthy exceptions include a recent estimate of the relative inclination ($i_{rel}$) of GJ 876 planets (Bean & Seifahrt 2009) and recent estimates for the line-of-sight inclinations ($i_{LOS}$) of the planets in HR 8799 (Lafrenière et al. 2009).

In an effort to remedy some of these issues and better describe system properties, investigators have been developing techniques to model RV data and to describe their orbital evolution. Goździewski et al. (2005) and Goździewski et al. (2008) utilize stability constraints and optimization techniques partly derived from the MEGNO (Mean Exponential Growth Factor for Nearby Orbits) method (Cincotta & Simó 2000). The advantages to MEGNO include simultaneous multi-planet fitting and efficient identification of quasi-periodic or irregular (chaotic) motion. A disadvantage is that the arbitrary choice of the "penalty" parameter determining this timescale prevents a rigorous interpretation of the results. Some authors (Ford 2005, 2006; Gregory 2007a,b) use Markov Chain Monte Carlo (MCMC) techniques to generate a sample of initial conditions from the posterior probability distribution. The strength of these techniques relies on rigorous Bayesian calculation and interpretations, and a weakness is that stability must be individually tested in each of a large number of models. For datasets that result in many unstable models,

Electronic address: veras@astro.ufl.edu
[1] Astronomy Department, University of Florida, 211 Bryant Space Sciences Center, Gainesville, FL 32111, USA

this procedure may result in a time-consuming and perhaps inefficient computational effort. Here, we follow the methodology of Veras & Ford (2009), which relies on MCMC-based simulations to derive ensembles of initial conditions.

We assume that the motion is described by a sum of Keplerian (i.e. non-interacting) orbits. Each ensemble of initial conditions consists of a list of masses, semimajor axes, eccentricities, arguments of pericenter, inclinations and nodes, assuming an initial mean anomaly for each planet. We then assign line-of-sight and relative inclinations to planets with these ensembles of orbital elements in order to sample from the entire phase space of possible initial conditions.

When planetary orbits are integrated forward in time, the system may exhibit a variety of evolutionary paths. Unrestricted planetary inclinations admit a wide variety of phase space regimes, often including those where apsidal and resonant angles circulate, librate and exhibit chaotic motions (Michtchenko et al. 2006b). In this work, because we consider systems containing two massive exoplanets with a wide range of eccentricities and inclinations, we must appeal to numerical integrations.

Here, we investigate the dynamical evolution of five two-planet systems which contain sufficiently numerous and accurate radial velocity orbital data suitable for a wide-ranging study. In §3, we show that the stability and dynamical properties of these systems can be significantly influenced by the initial values of $i_{rel}$ and $i_{LOS}$. Four of these systems are "hierarchical", meaning they contain large ratios of orbital distances, which often include a close-in planet whose evolution could be affected by the general relativistic precession of the pericenter. We aim to characterize the eccentricity variation, stability, secular effects and resonant signatures of planets in these systems as a function of $i_{rel}$ and $i_{LOS}$, while taking into account the uncertainties of the measured orbital parameters for each planet. We combine investigations of the hierarchical HD 12661 with the system studied here to draw inferences for effective methods of future dynamical investigations of hierarchical systems, and to determine their general evolutionary trends (such as the propensity, or lack thereof, for planets to periodically attain circular orbits; Barnes & Greenberg 2006a,b).

We describe our methodology in §2, and present the results of the N-body simulations in §3. Tables 2-14 present summary statistics, two or three tables per system, arranged by row according to the binned relative inclination between both planets; the accompanying figures help the reader visualize the data. We discuss the results in §4 and conclude in §5.

## 2. METHODS

The setup of our simulations closely follows that of Veras & Ford (2009). First, we generate a sample of initial conditions that will serve as the basis for numerical integrations.

Using RV data from Wright et al. (2008), we utilize the MCMC analysis methods and prior distributions from Ford (2006). In particular, we calculate 5 Markov chains each containing $10^5$ or $10^6$ states per system. Each state includes the orbital period ($P$), velocity amplitude ($K$), eccentricity ($e$), argument of pericenter measured from the plane of the sky ($\omega$), and mean anomaly at a given epoch ($u$) for each planet specified by subscripts. We randomly select 13 sets of 500 states, where each set is restricted to a particular range of $i_{rel}$. We sampled from a uniform distribution for the longitude of ascending nodes, $\Omega$, and from an isotropic distribution for the $i_{LOS}$ of each planet. Then we used rejection sampling to choose 500 isotropically distributed pairs of $i_{LOS}$ values in each of 13 $i_{rel}$ bins. The planet masses, $m$, and semimajor axes, $a$, are obtained from each set of $(P, K, e, \omega, i, \Omega, u)$ values from relations derived with a Jacobi coordinate system (Lee & Peale 2003). The 13 $i_{rel}$ bins are split into one coplanar bin and 12 bins which contain systems with relative inclinations in 15° intervals from 0° to 180°. We used stratified sampling to obtain sufficiently large samples at both low and high inclinations.

Second, we perform integrations to test each set of initial conditions for long-term stability. We integrated each set of initial conditions with the hybrid symplectic integrator of `Mercury` (Chambers 1999) for 1 Myr, and obtained snapshots of the system states every $10^3$ yr. Inspection of a representative sample of stable configurations reveals that 1 Myr typically exceeds secular timescales.

We assume that the actual systems will not undergo instability immediately ($< 10^6$ yr), and generate a subsample of initial conditions that do not show indications of instability during our simulations. We classified systems as "unstable" if, for either planet, $(a_{\max} - a_{\min})/a_0 > \tau a_0$, where $a_{\max}$, $a_{\min}$ and $a_0$ represent the maximum, minimum and initial values of the semimajor axis, and $\tau = 0.3$. Additionally we consider systems which have undergone a close encounter (where two bodies come within a Hill radii of one another) or collision to be unstable. Our criterion may not identify a small fraction of some systems that will manifest instability on longer timescales, but importantly it also avoids miscategorizing a system exhibiting bounded chaos as unstable (e.g., Goździewski 2003).

In addition to testing for stability, we compute the extent to which planets' eccentricities and mutual relative inclination vary over the course of the simulations and for what fraction of the planets' eccentricity and inclination exceed their initial values. We also determine how closely the planetary orbits approach circularity by computing $\kappa_b \equiv e_{b,min}/e_{b,max}$, where $e_{b,min}$ and $e_{b,max}$ represent the minimum and maximum eccentricities attained throughout a simulation for planet $b$. A similar definition holds for planet $c$. If $\kappa \approx 0$, a planet's eccentricity will periodically approach zero.

For two planets on nearly planar orbits, the difference of the longitude of periapses, $\Delta\varpi$, has dynamical significance (Chiang et al. 2001; Chiang & Murray 2002; Beaugé et al. 2003; Ji et al. 2003; Zhou & Sun 2003; Namouni 2005; Migaszewski & Goździewski 2009). In the planar case, when this difference is 0° (180°), the planetary orbits are said to be "aligned" ("anti-aligned"). An "Apsidal Corotation Resonance" (ACR; Beaugé & Michtchenko 2003; Ferraz-Mello et al. 2003; Lee 2004; Kley et al. 2005; Beaugé et al. 2006; Michtchenko et al. 2006a; Voyatzis & Hadjidemetriou 2006; Sándor et al. 2007; Michtchenko et al. 2008a,b) refers to system evolutions that result in $\Delta\varpi$ librating about 0° or 180° and can result from either purely secular evolution or secular plus resonant interactions.

However, for nonzero inclinations, the angle between the pericenter directions deviates from $\Delta\varpi$ in the planar case. The most natural plane on which to measure three-dimensional dynamics is the invariable plane. Therefore, for each snapshot in time and for each N-body integration, we measure $\Delta\varpi'$, the difference of the longitude of pericenters after projecting onto the invariable plane. A time series of these measurements of $\Delta\varpi'$ over a period of time, $t_0$, sometimes reveals either "circulation," or "libration" about a particular value, the "libration center," $l_0$. Strictly, an angle librates if there is a range of values that the angle avoids; $l_0$ is then the middle value of the range *not* avoided by the angle. Unless the angle is continuously sampled, there will always be a finite range avoided by the angle. Therefore, because of finite sampling from integration output, we consider $\Delta\varpi'$ to librate if every value of $\Delta\varpi'$ over a time $t_0$ avoids a range larger than 90°. The location of this range depends on the value of $l_0$ considered.

When testing for libration, we consider a putative value of $l_0$ and determine if every value of $\Delta\varpi'$ is contained in the range from $l_0-135°$ to $l_0+135°$. If an angle librates, investigators often report a libration amplitude about $l_0$. Veras & Ford (2009) utilize two alternative variation measures, the root mean square deviation and mean absolute deviation, which are more robust than the amplitude given finite sampling and additional short-term perturbations. We calculate the RMS deviation of $\Delta\varpi'$ about each of $l_0 = (0°, 90°, 180°, 270°)$. Our choice of $l_0$ includes each of the common libration centers. Analytical considerations (Murray & Dermott 1999; Morbidelli 2002) demonstrate that $l_0 = 0°$ and $l_0 = 180°$ ("symmetric solutions") are the only possiblities for purely secular evolution, and numerous numerical studies of aligned and anti-aligned configurations bear this trend out. However, $l_0$ may take on other values ("asymmetric solutions"; Beauge 1994; Winter & Murray 1997; Jancart et al. 2002; Beaugé et al. 2003; Murray-Clay & Chiang 2005) if a system is near a mean motion resonance. Of the systems considered here, only HD 108874 is near a MMR. Assuming the system is not undergoing asymmetric libration and considering a few alternative values of $l_0$ (e.g., 90° and 270°) allows us to estimate the frequency of systems being misclassified.

## 3. RESULTS

### 3.1. *Common Attributes*

Wright et al. (2008) provide best-fit orbital solutions to radial velocity observations of multiplanet systems. Our calculations are based on the posterior probability distribution for orbital parameters described in Section 2. Here, we give an approximate summary of system properties. In all systems except HD 190360, planet $b$ is the inner planet. The ratio of semimajor axes nearly exceeds one order of magnitude in HD 11964 ($a_b, a_c \approx 0.2, 3.2$ AU), HD 38529 ($a_b, a_c \approx 0.1, 3.7$ AU), HD 168443 ($a_b, a_c \approx 0.3, 2.9$ AU), and HD 190360 ($a_c, a_b \approx 0.1, 3.9$ AU), and approximately corresponds to the 4:1 Mean Motion Resonance (MMR) in HD 108874 ($a_b, a_c \approx 1.1, 2.7$ AU). Assuming coplanarity, The outer planet is more massive in HD 11964 ($M_b \sin i_{b,LOS}, M_c \sin i_{c,LOS} \approx 0.1, 0.7 M_{\rm Jup}$), HD 38529 ($M_b \sin i_{b,LOS}, M_c \sin i_{c,LOS} \approx 0.8, 13 M_{\rm Jup}$), HD 168443 ($M_b \sin i_{b,LOS}, M_c \sin i_{c,LOS} \approx 8, 18 M_{\rm Jup}$), and HD 190360 ($M_c \sin i_{c,LOS}, M_b \sin i_{b,LOS} \approx 0.06, 1.5 M_{\rm Jup}$), whereas the planet masses are comparable in HD 108874 ($M_b \sin i_{b,LOS}, M_c \sin i_{c,LOS} \approx 1.4, 1.0 M_{\rm Jup}$). In the limit that a planet's orbit is seen face-on, the planet's mass diverges and the corresponding system becomes unstable. However, most orbital orientations with respect to the Earth yield actual planet masses less than twice the observed mass; a planet's true mass exceeds its observed mass by at least one order of magnitude only if the planet's orbit is within $\approx 5.8°$ of being face-on. The currently observed orbital eccentricities of all the planets studied here vary from nearly circular ($\approx 0.01$) to significantly eccentric ($\approx 0.53$).

Libert & Henrard (2007) analyzed the proximity of particular multi-planet systems to strong mean motion resonance and found that HD 38529, HD 168443, HD 190360 are dominated by non-resonant motions. For HD 11964, the semimajor axis ratio of both planets typically exceeds 10, so a mean motion resonance is unlikely to dominate the evolution of that system. Of the 5 systems studied, only HD 108874 is near a mean motion resonance of order $\lesssim 10$.

### 3.2. *Non-Keplerian Effects*

Because some of the above planets harbor semimajor axes of just a few tenths of an AU, we must consider the possible effects on the dynamics due to the pericenter precession caused by GR (Ford et al. 2000; Adams & Laughlin 2006a,b). This precession is the most significant deviation from a Keplerian orbit at these orbital periods and we use the standard approximation (Fabrycky & Tremaine 2007):

$$\dot{\omega}_{\rm GR} = \frac{3G^{3/2}\left(M_\star + M_{\rm inner}\right)^{3/2}}{a_{\rm inner}^{5/2} c^2 \left(1 - e_{\rm inner}^2\right)} \approx \frac{3GM_\star}{a_{\rm inner} c^2 \left(1 - e_{\rm inner}^2\right)} n_{\rm inner}, \quad (1)$$

where $n$ refers to the mean orbital motion, $c$ the speed of light, $M_\star$ the mass of the star, and where the subscripts "inner" and "outer" will henceforth refer to the inner and outer planets. In order to assess the possible effect of GR on our simulations, we can compare the value of $\dot{\omega}_{\rm GR}$ with the magnitude of the precession caused by secular evolution with the outer planet (Zhou & Sun 2003):

$$\dot{\omega}_{\rm sec} = \sqrt{(y_1 - y_2)^2 + 4 y_1 y_2 \left(\frac{b_{3/2}^{(2)}}{b_{3/2}^{(1)}}\right)^2} \quad (2)$$

where

$$y_1 = \frac{1}{4} \frac{M_c a_b^{-3/2}}{\sqrt{M_\star + M_b}} \alpha^2 b_{3/2}^{(1)}(\alpha) \quad (3)$$

$$y_2 = \frac{1}{4} \frac{M_b a_c^{-3/2}}{\sqrt{M_\star + M_c}} \alpha b_{3/2}^{(1)}(\alpha) \quad (4)$$

and $b_s^{(j)}(\alpha)$ are Laplace coefficients, with $\alpha$ representing the semimajor axis ratio such that $\alpha < 1$. Equation (2) is derived based on Laplace-Lagrange secular theory, accurate to second-order in the eccentricities. The planetary eccentricities in our simulations may attain values

close to unity, and higher-order expansions do not admit eigenvalue solutions such as those from Eq. (2) (see, e.g., Veras & Armitage 2007). Further, by definition, secular theory assumes constant semimajor axes. Hence, the estimate of $\dot{\omega}_{\rm sec}$ for potentially near-resonant systems such as HD 108874 may be inaccurate.

With the above caveats in mind, the ratio of these two precession rates, $\chi_{\rm sec} \equiv \dot{\omega}_{\rm sec}/\dot{\omega}_{\rm GR}$, provides a measure of the importance of GR in a system. Table 1 lists values of $\chi_{\rm sec}$ for representative values of orbital parameters and masses of all systems studied. Because $\chi_{\rm sec} \gg 1$ only for HD 168443 and HD 108874, general relativity may play a significant role in the dynamics in HD 11964, HD 38529 and HD 190360. Therefore, we explicitly add into Mercury the effect of GR according to the approximation in Eq. (1) for calculating an additional set of 6500 simulations for each of the three systems.

For highly inclined systems, a planet may undergo coupled inclination and eccentricity oscillations through a secular exchange of angular momentum, known as Kozai oscillations. Kiseleva et al. (1998) gives the period for these oscillations – the "Kozai period" – as:

$$P_{\rm Koz} = \frac{2P_{\rm outer}^2}{3\pi P_{\rm inner}} \frac{M_\star + M_{\rm inner} + M_{\rm outer}}{M_{\rm outer}} \left(1 - e_{\rm outer}^2\right)^{3/2}. \quad (5)$$

Because this period refers to the oscillations of the inner planet's argument of pericenter, the relative contribution of the Kozai mechanism to GR can be expressed as: $\chi_{\rm Kozai} \equiv \dot{\omega}_{\rm Kozai}/\dot{\omega}_{\rm GR} = 2\pi/P_{\rm Koz}\dot{\omega}_{\rm GR}$. Table 1 reports representative values of $\chi_{\rm Kozai}$ for each system studied here. The values demonstrate that the Kozai mechanism could be significant (if the relative inclination exceeds $\approx 40^\circ$) for HD 168443 and HD 108874, the two systems where secular perturbations from the outer planet dominates the effect of GR.

Other possibly significant effects for Hot Jupiters are tidal deformation and stellar oblateness. In order to assess the magnitude of these additional effects, we derive ratios from the expressions given by Jordán & Bakos (2008):

$$\chi_{\rm tide} \equiv \frac{\dot{\omega}_{\rm tide}}{\dot{\omega}_{\rm GR}} \approx 0.51 \left[\frac{1 + (3/2)e_{\rm inner}^2 + (1/8)e_{\rm inner}^4}{\left(1 - e_{\rm inner}^2\right)^4}\right] \times \left(\frac{M_{\rm Jup}}{M_{\rm inner}}\right) \left(\frac{0.05{\rm AU}}{a_{\rm inner}}\right)^4 \left(\frac{R_{\rm inner}}{R_{\rm Jup}}\right)^5, \quad (6)$$

$$\chi_{\rm obl} \equiv \frac{\dot{\omega}_{\rm obl}}{\dot{\omega}_{\rm GR}} \approx 0.021 \left(1 - e_{\rm in}^2\right) \times \left(\frac{0.05{\rm AU}}{a_{\rm in}}\right) \left(\frac{J_2}{10^{-6}}\right) \left(\frac{M_\odot}{M_\star}\right) \left(\frac{R_\star}{R_\odot}\right)^2, \quad (7)$$

where $R_\star$ refers to the radius of the star and $J_2$ is a oblateness constant present in the typical expression for gravitational potential (e.g., Eq. 6.218 of Murray & Dermott 1999). Both ratios $\chi_{\rm tide}$ and $\chi_{\rm obl}$ are only weakly dependent on the eccentricity of the inner planet. The ratios can be estimated only in a rough sense because of the generally unknown stellar $J_2$ for the former and because of the unknown radii of several planets and the strong dependence on $R_{\rm inner}$ for the latter. Further, for $\chi_{\rm tide}$, not shown are the dependencies on the internal structures of both the star and planet, which are unknown. Table 1 lists estimates for the *initial* values of these ratios by adopting $J_2 = 2 \times 10^{-7}$ (Pireaux & Rozelot 2003) and assuming $R_{\rm inner} \sim R_{\rm Jup}$. In almost all cases, $\chi_{\rm tide} << 1$ and $\chi_{\rm obl} << 1$, so GR precession will dominate over tides and the effects from stellar oblateness. The only possible exception is for HD 190360, with $\chi_{\rm tide} = 0.21$. Hence, we neglect these latter two effects in our simulations.

### 3.3. *System Stability*

For all systems except HD 168443, over 95% of the nearly coplanar systems, in both the prograde and retrograde sense, remained stable over 1 Myr. Largely independent of each planet's line-of-sight inclination, all systems demonstrate that as the relative inclination between both planets approaches 90°, the systems become increasingly likely to undergo instability. Figure 1 graphically depicts the fraction of systems which remain stable over 1 Myr for all five systems. This figure broadly quantifies the effect that GR has on stabilizing systems with a close ($a \lesssim 0.1$ AU) planet.

When Kozai oscillations are present, the maximum eccentricity achieved by the inner planet ($e_{\rm inner,max}$) is lower in our numerical simulations which include GR than in the simulations which do not include GR. The Kozai mechanism induces angular momentum transfer which causes the inner planet's eccentricity, inclination and argument of pericenter to evolve. Because these effects are coupled, when GR causes a change in the rate of argument of pericenter, the effect affects the planet's eccentricity as well. Both Lin et al. (2000) and Fabrycky & Tremaine (2007) relate the Kozai timescale, general relativistic precession, and $e_{\rm inner,max}$ through:

$$\cos^2 i_{\rm rel,0} = \frac{3}{5}\left(1 - e_{\rm inner,max}^2\right) - \frac{2}{5}\left[\left(1 - e_{\rm inner,max}^2\right)^{-1/2} + 1\right]^{-1} \left(\frac{2\pi}{\chi_{\rm Kozai}}\right)\Bigg|_{e_{\rm inner,0}=0} \quad (8)$$

assuming that the inner planet is on an initially circular orbit and where the "0" subscript will henceforth refer to an initial value. We have generalized this equation to include an initial non-zero eccentricity (see the Appendix and Eqs. 6-7).

Equation (8) demonstrates that for an initial relative inclination high enough to trigger the Kozai mechanism, the maximum eccentricity of the inner planet decreases as $\dot{\omega}_{GR}$ increases. Hence, a high value of $\dot{\omega}_{GR}$ provides a stabilizing mechanism for a system.

We test the quality of the analytical approximation afforded by Eq. (6) by using our simulation output. Applying the values in Table 1 to Eq. (7) illustrates that for all systems except HD 190360, the inner planet's maximum eccentricity should not be reduced by GR and Kozai effects. Fig. 2 plots this eccentricity difference vs. the initial relative inclination for simulation data (dots) and Eq. (6) (solid line) for HD 11964. The curve in Fig. 2 is based on a single representative value of $\chi_{\rm Kozai}$; in reality, each dot corresponds to a different curve. The dots are generally below by the curve given in the analytical model, as expected.

The relative contribution of Kozai-like oscillations can be identified by the libration of the argument of pericen-

ter of the inner planet ($\omega_{\rm inner}$). Asymmetric libration of this angle, particularly about the values 90° and 270°, is characteristic of the Kozai mechanism. Therefore, we compute the fraction of inner planet argument of pericenters measured *with respect to* (as opposed to projected on) the invariable plane, for all systems.

HD 108874 and HD 168443 perhaps best demonstrate the interplay between these angles because for those systems (one near-resonant and one far from strong MMR), $\chi_{\rm Kozai} \gg 1$. Figures 3-4 illustrate the fraction of systems where $\Delta\varpi'$ librates about 0° (blue/dotted lines with triangles) or 180° (red/dashed line with squares), and where $\omega_b$ librates around 90° or 270° (black/solid line with dots). Prograde and retrograde coplanar systems predominately demonstrate antialignment and alignment of $\Delta\varpi'$, respectively, for HD 108874, and alignment only in HD 168843. The solid lines peak as $i_{\rm rel}$ approaches 90°. Therefore, the Kozai mechanism has a significant effect at large relative inclination values, as demonstrated by the asymmetric libration of $\omega_b$. This libration would be masked by considering libration of $\Delta\varpi'$ alone, which would instead suggest that about half of the systems show alignment and the other half show antialignment at high relative inclinations.

### 3.4. *HD 11964*

Butler et al. (2006) announced the existence of the multiple planet system around HD 11964. Soon after, Gregory (2007b) performed a Bayesian analysis of the same data and presented evidence for a third planet (of $\sim 0.21 M_J$) in the system at $\sim 1.1$ AU. This planet's existence would imply an unusually small jitter of less than 0.9 m/s. Further, it would require that the commensurability with a one year period is not the result of aliases with the annual observing pattern and/or imprecise barycentric correction (Baluev 2008). Therefore, there is only strong evidence for two planets given the current data, and we consider the dynamics of two-planet solutions.

We ran 6500 N-body integrations of HD 11964 including GR and 6500 integrations not including GR. We present the simulation output in Tables 3 and 10. Table 3 indicates: 1) The median amplitude of the outer planet's current eccentricity does not exceed 0.075 for any inclination. The value of $\kappa_c$ ($\equiv e_{c,min}/e_{c,max}$), indicates that the eccentricity variation achieved throughout the simulation is modest; $\kappa_c \geq 0.83$ in all cases with GR. Regardless of the system's initial orientation, the planet's orbit does not become significantly more circular during its secular evolution. 2) In the coplanar prograde and retrograde (general relativistic) cases, the eccentricity evolution is quite modest (e.g. $\kappa_b \approx 0.92(0.95), 0.89(0.93)$ and $\kappa_c \approx 0.92(0.94), 0.93(0.93)$). 3) We find no indication of instability except when $60° < i_{\rm rel,0} < 120°$. When $i_{\rm rel}$ approaches 90°, the eccentricity of the inner planet begins to vary drastically. Incorporating GR precession decreases the inner planet's eccentricity variation enough to nearly double the fraction of stable systems when $60° < i_{\rm rel,0} < 75°$ and $105° < i_{\rm rel,0} < 120°$, and quintuple the fraction of stable systems when $75° < i_{\rm rel,0} < 105°$.

Table 10 indicates: 4) In the coplanar prograde and retrograde cases, $\Delta\varpi' > 90°$, indicative of large amplitude libration (regardless of the inclusion of GR). 5) About three-quarters of systems with $45° < i_{\rm rel,0} < 75°$ and $105° < i_{\rm rel,0} < 135°$ demonstrate asymmetric libration of $\omega_b$, indicating that the Kozai mechanism does play a significant role at these high relative inclinations. 6) Secular perturbations lead to complex dynamics at both low and high inclinations. For moderate relative inclinations ($30° < i_{\rm rel,0} < 45°$, $120° < i_{\rm rel,0} < 135°$), $\Delta\varpi' \approx 64°$ and is just as likely to librate about $0°, 180°$, or some other value. These relative inclinations produce large RMS amplitudes, and in the prograde case, demonstrate preferential alignment of $\Delta\varpi'$.

### 3.5. *HD 38529*

The planet HD 38529 b was announced in Fischer et al. (2001) and the outer planet (HD 38529 c) was confirmed in Fischer et al. (2003). HD 38529 c has a minimum mass within tenths of a Jupiter mass of the oft-cited 13 $M_{\rm Jup}$ cutoff. In addition to orbiting planets, the host star exhibits IR excess, indicating the presence of a cool disk at wide separations (Moro-Martín et al. 2007).

Tables 5 and 11 summarize the results of all 13,000 simulations for HD 38529. The first two tables demonstrate: 1) For relative inclinations within 60° of coplanarity, the vast majority of systems are stable. 2) Almost all systems that are within 15° of $i_{\rm rel,0} = 90°$ become unstable when neglecting GR; including GR increases the number of stable systems by over a factor of 50 to $11\% - 14\%$. 3) The outer planet's eccentricity remains relatively constant (to within 10%) in all GR-based cases (and all non-GR-base cases except for $i_{rel,0}$ values closest to 90°). Recall that GR primarily contributes to the pericenter change of the *inner* planet. Hence, the effect on the outer planet is indirect, yet non-negligible at high relative inclinations. 4) The eccentricity variation of the inner planet increases gradually as $i_{\rm rel,0}$ approaches 90°. Including GR slightly decreases the variability of the inner planet's eccentricity. 5) For highly inclined, stable systems, the relative inclination can vary from less than 90° (prograde) to greater than 90° (retrograde).

Regarding libration properties, Table 11 illustrates: 6) The RMS deviations of $\Delta\varpi'$ are high enough to be consistent with circulation in all relative inclination bins, 7) Assuming libration of $\Delta\varpi'$, alignment is strongly preferred in the coplanar prograde and retrograde cases. 8) GR's primary effect on the libration of $\Delta\varpi'$ is to cause preferential alignment of the angle at moderate relative inclinations ($45° \leq i_{\rm rel,0} \leq 75°$ and $105° \leq i_{\rm rel,0} \leq 135°$). 9) For these values of $i_{\rm rel,0}$, asymmetric libration of $\Delta\varpi'$ is dominant, indicating the role of the Kozai mechanism.

### 3.6. *HD 108874*

HD 108874's two known planets (Vogt et al. 2002, 2005) have a orbital period ratio close to four, suggesting that they may be in or near a 4:1 MMR (Goździewski et al. 2006; Libert & Henrard 2007). Our joint statistical and dynamical analysis is well suited to testing this possibility. First, we performed a standard MCMC analysis assuming that each planet traveled on an independent Keplerian orbit. As for the previous planetary systems, we used the standard MCMC output to generate ensembles of initial conditions for N-body integrations to test for dynamical stability and secular evolution of the eccentricity and inclinations. In principle, these results might be affected by the planet-planet

interactions, particularly if the two planets are in a mean-motion resonance. Therefore, we performed a second analysis using full N-body integrations for both the statistical and dynamical analyses. The prior probability distributions were similar to those in our previous analysis with non-interacting planets. In other words, the priors are based on the period and velocity amplitude inferred from the Jacobi orbital elements. We adopt a stellar mass of $0.95 M_{\odot}$. Since the relative orientation of the orbits matters for the N-body simulations, we must add priors for the inclination of the orbital plane and longitude of nodes (where the orbit punctures the sky plane). We consider both: 1) a prograde coplanar configuration with an isotropic prior for the inclination of the system (i.e., a common inclination and a common longitude of ascending node for each system), or 2) an isotropic prior for the inclination of each orbit and a uniform prior for the line of nodes. As before, we select subsets of the output based on the relative inclination to be used for long-term N-body simulations to investigate stability and secular eccentricity and inclination evolution. The likelihood is evaluated based on comparing observations and the simulated stellar velocities (in a barycentric frame) evaluated at the time of each radial velocity observation.

We again employ Markov chain Monte Carlo (MCMC) to sample from the posterior probability distribution for the masses and orbital parameters. The convergence rate of MCMC is often sensitive to the algorithm for proposing the next state (e.g., candidate transition probability distribution function). When performing Bayesian analysis with N-body interactions, we replace the Gaussian random walk Metropolis algorithm adapted for analyzing radial velocity data sets (Ford 2006) with a differential evolution Markov chain Monte Carlo algorithm (DEMCMC; ter Braak 2006). In this algorithm, each state of the Markov chain consists of an ensemble of initial conditions (known as a generation). For our analysis of HD 108874, each generation consisted of an ensemble of 1,024 sets of initial conditions. For the initial generation, the initial conditions were drawn from a posterior sample calculated assuming independent Keplerian orbits (i.e., using the standard MCMC approach; Ford 2006). For each of $10^5$ subsequent generations, 1,024 new sets of initial conditions are proposed, based on combinations of multiple sets of initial conditions from the previous generation. The acceptance probability is chosen so as to converge to the desired posterior probability distribution. As before, we perform long-term N-body integrations for a subset of the initial conditions drawn from the latter portions of the Markov chain.

The results of the DEMCMC+N-body analysis (including planet interactions) and the standard MCMC analysis (assuming independent Keplerian orbits) are extremely similar (Table 6 For example, for coplanar, prograde systems, the MCMC (DEMCMC+N-body) analysis estimates the fraction of stable systems to be 97.6% (99.0%). Similarly, the statistics describing the extend of eccentricity evolution are $\kappa_b = 0.29$ (0.29) and $\kappa_c = 0.25$ (0.26). Thus, we conclude that our results for HD 108874 are not sensitive to the effects of short-term planet-planet interactions or the assumption of independent Keplerian orbits. The exception is when $\sin i$ becomes small. However, if $\sin i$ is small enough to cause significant short-term interactions, then the system is very likely to be rejected based the test for orbital stability.

In order to explore the possibility of the system being in resonance, we perform a systematic search for the possible libration of all resonant angles associated with the 4:1, 7:2, 11:3, and 15:4 MMRs. These commensurabilities were chosen based on their proximity to an orbital period ratio of four. Each resonant angle has the form

$$\phi = j_1 \lambda_{\rm out} + j_2 \lambda_{\rm in} + j_3 \varpi_{\rm out} + j_4 \varpi_{\rm in} + j_5 \Omega_{\rm out} + j_6 \Omega_{\rm in}, \quad (9)$$

where $\lambda$, represents the mean longitude, $\varpi$ represents the longitude of pericenter, and $j_i$ are constants. We sample four MMRs, up to order 11, in case any high- ($> 10$) order resonances may play a role in the system's dynamical evolution (Michtchenko et al. 2006b). For each of the four MMRs, all combinations of $j_i$ are considered such that $\sum j_i = 0$ and $(j_5 + j_6)$ is even. We performed this search for all 6,500 systems simulated for HD 108874. We flagged any angles which librated for at least $t_0 = 10^5$ yr. We discovered that less than 0.5% of all simulations studied exhibited libration, and even then only for a few $10^5$ yr. There is no apparent correlation with resonance and stability nor resonance and initial relative inclination. Thus, HD 108874 is very unlikely to be in resonance based on the current RV data.

Regardless of the possible influence of resonant or near-resonant terms, the characteristics of the secular evolution (Table 6) are striking: 1) Despite a median initial planet $b$ eccentricity of $\approx 0.12$, $\kappa_b < 0.30$ for every relative inclination bin, and approaches zero as $i_{\rm rel,0}$ approaches 90°, 2) For $i_{\rm rel,0} = 40° - 75°$, the eccentricity of the planetary orbits approaches zero, 3) Unlike for the inner planet's orbit, the outer planet's orbit demonstrates an increasingly restrictive eccentricity range in the retrograde case as the planets' orbits become coplanar. The values in Table 12 reveal other interesting aspects of the motion: 4) $\Delta\varpi'$ always demonstrates symmetric libration, regardless of $i_{\rm rel,0}$. 5) Prograde coplanar systems are almost entirely anti-aligned, whereas retrograde coplanar systems are entirely aligned. This shift from aligned to anti-aligned could indicate a significant contribution from near-resonant terms even though the planets are not strictly locked in a MMR. 6) Prograde coplanar systems feature the smallest libration amplitudes. 7) As demonstrated in Fig. 3, the system evolution exhibits libration of $\omega_b$ in a robust Kozai-like fashion for $40° < i_{\rm rel,0} < 140°$ except for the unstable systems prevalent in the $90° < i_{\rm rel,0} < 120°$ regime.

### 3.7. *HD 168443*

After the discovery of HD 168443 b (Marcy et al. 2001), Udry et al. (2002) found a companion brown dwarf in the system. Veras & Armitage's (2007) numerical integrations of the system, assuming coplanarity, demonstrate that both planets undergo significant eccentricity evolution. They found that the two most apparent modulation frequencies are $\sim 10^3$ yr and $\sim 10^4$ yr, and that the apsidal angle clearly circulates.

Our 6,500 simulations of this system are summarized in Tables 7 and 13. Table 7 demonstrates: 1) Almost no stable systems can exist for $60° \leq i_{\rm rel,0} \leq 120°$ and few systems remain stable when this range is extended by 15° in each direction. 2) At least 20% of all systems become

unstable for every relative inclination bin except for the perfectly coplanar case, where 13.0% of the systems sampled become unstable. 3) For the vast majority of stable systems, planet $c$'s eccentricity variation is independent of the relative inclination. 4) For highly inclined, stable systems, the relative inclination can vary from less than 90° (prograde) to greater than 90° (retrograde). Table 13 shows that: 5) For all relative inclinations, the libration amplitude of $\Delta\varpi'$ exceeds 90°, 6) $\Delta\varpi'$ is nearly always preferentially aligned and 7) $\omega_b$ exhibits strong Kozai-like behavior for $i_{\rm rel,0}$ values just under 60° and just over 120°.

### 3.8. *HD 190360*

Udry et al. (2003) announced a planet in HD 190360 and Vogt et al. (2005) and Goździewski & Migaszewski (2006) followed up with a detection and confirmation of an additional planet whose mass is approximately one Neptune-mass. Primarily because of the inner planet's small semimajor axis, GR has the greatest effect on this system (see Table 1).

Tables 8, 9 and 14 provide the summary output from the system's 6,500 GR-based and 6,500 non-GR-based simulations. Table 8 demonstrates: 1) An appreciable fraction of stable systems exist for all relative inclinations. However, for $60° \leq i_{\rm rel,0} \leq 120°$, $\approx 89\%$ of systems without GR are unstable. Including GR, however, stabilizes *nearly every one* of those systems. 2) The outer planet's eccentricity varies by less than 1% in the vast majority of individual stable systems. 3) The presence of GR reduces the variation of the inner planet's eccentricity by up to a factor of 4.

Table 14 suggests: 4) Without GR, the lowest libration amplitudes and the highest amplitude standard deviations of $\Delta\varpi'$ occur when the relative inclination is $15° - 30°$ offset from either the prograde or retrograde planarity. Including GR results in different conclusions; the system does not demonstrate small libration amplitudes nor asymmetric libration of $\Delta\varpi'$. 5) In the coplanar and retrograde planar cases, alignment of $\Delta\varpi'$ is preferred over anti-alignment by a factor of nearly four. 6) With the presence of GR, the libration amplitudes all exceed 90°, commensurate with circulation. 7) The Kozai signatures are weaker than in any other system, corroborating the trend exhibited by the values of $\chi_{\rm Kozai}$ from Table 1.

### 3.9. *HD 12661*

Veras & Ford (2009) performed a similar MCMC-based statistical analysis for HD 12661, but with broader relative inclination bins. For completeness, we compare some of their results with the outcomes presented here. HD 12661 is a two planet system where the inner (outer) planet properties are: $M \approx 2.3 M_{\rm Jup} (1.8 M_{\rm Jup})$, $a \approx 0.8$AU$(2.4$AU$)$, and $e \approx 0.35(0.05)$. The authors demonstrated that the outer planet spends over $\sim 96\%$ of the time following an orbit that is more eccentric than the one currently observed. In the coplanar prograde case, all systems were stable, and in the coplanar retrograde case, almost all systems were stable. 16.4% of systems remained stable for $60° \leq i_{\rm rel,0} \leq 90°$, whereas only 0.2% did so for $90° \leq i_{\rm rel,0} \leq 120°$. This asymmetry about 90° is significant and much greater than the slight asymmetries about 90° seen for HD 11964, HD 38529, and HD 190360, but comparable to those in HD 108874. Further, the alignment of $\Delta\varpi'$ for HD 12661 shows a strong dependence on $i_{\rm rel,0}$; only $\approx 33\%$ of coplanar prograde systems show alignment of $\Delta\varpi'$, whereas $\approx 99.4\%$ of coplanar retrograde systems show alignment. The only system studied here with a similar trend is HD 108874, whose $\Delta\varpi'$ is nearly entirely antialigned in the prograde coplanar case, and entirely aligned in the retrograde coplanar case.

## 4. DISCUSSION

Hierarchical systems can be highly eccentric or inclined (or even retrograde). Such large eccentricities and inclinations imply that numerical integrations are often necessary to model the dynamics of extrasolar systems. Analytical treatments of two-planet evolution abound (e.g. Murray & Dermott 1999; Morbidelli 2002, and references therein), and often rely on approximations to the gravitational potential, known as "disturbing functions," The Laplace expansion of the disturbing function (Ellis & Murray 2000) relies on a Taylor expansion about zero eccentricities and inclinations and is limited in eccentricity by the Sundman criterion (Ferraz-Mello 1994; Šidlichovský & Nesvorný 1994). Although effective for small Solar System bodies, this disturbing function must be used with care with respect to extrasolar planets (Veras 2007). Beaugé (1996) and Beaugé & Michtchenko (2003) developed a high eccentricity version of a disturbing function in the planar case which can reliably model the evolution of massive extrasolar planets with eccentricities up to $\approx$ 0.5. Because quadrupole and octopole expansions are in terms of the semimajor axis ratio, their accuracy is diminished for weakly hierarchical systems. For non-coplanar systems, one can use semi-numerical averaging (Michtchenko & Malhotra 2004; Michtchenko et al. 2006b; Migaszewski & Goździewski 2009) or adaptions of Gauss' method (Touma et al. 2009), which are valid for high $e$ and $I$. However, these studies neglect resonant and short-term perturbations. We find that these can be significant for some planetary systems, even if not in MMR (e.g. HD 108874).

We can compare our secular evolution results with those from other investigators. Barnes & Greenberg (2006b) performed a dynamical study of 2-planet systems which did not incorporate uncertainties in the initial conditions and assumed that each system was coplanar and edge-on. With those assumptions, they found that several of these systems had at least one eccentricity that periodically obtains a small value. They claimed that an unexpectedly high frequency of systems with "near separatrix motion" implied that this property couldn't be due to planet scattering from initially circular orbits. Instead, we find that once we 1) focus our attention on two-planet systems with published RV data and significant secular evolution, 2) avoid systems near MMRs, and 3) account for the uncertainties in the current orbital elements, only a modest fraction show significant secular eccentricity evolution with one planet returning to a near circular orbit for all viable inclinations. This fraction is equal to 2/6500 for HD 11964, 1/6500 for HD 38529, 757/6500 for HD 108874, 27/6500 for HD 168443, and 0/6500 for HD 190360, assuming that the planet which returns to or stays on a near circular orbit achieves an

eccentricity 1) range of at least 0.1, and 2) between 0.01 and 0.05 at least once every $5 \times 10^4$ yrs. For HD 108874, if we specify that the eccentricity range must be at least 0.2, then the fraction becomes 488/6500.

In particular, Fig. 5 plots the value of $\kappa$ for the five systems analyzed here as a function of initial $i_{\rm rel,0}$. The figure demonstrates that the eccentricity variation of the inner planet typically increases as the initial $i_{\rm rel,0}$ approaches 90°, and that $\kappa$ can take on values from $\sim 0.10 - 0.90$. Barnes & Greenberg (2006b) use a measure, $\epsilon \equiv 2\min(\sqrt{u^2+v^2})/(u_{\rm max} - u_{\rm min} + v_{\rm max} - v_{\rm min})$, where $u \equiv e_{\rm inner} e_{\rm outer} \sin(\Delta\varpi)$ and $v \equiv e_{\rm inner} e_{\rm outer} \cos(\Delta\varpi)$ to compare the minimum eccentricity value of either planet attained during evolution to the range of variation, assuming the planetary orbits are coplanar. Their value of $\epsilon$ for the near-MMR system HD 108874 (0.198) is comparable to the value of $\kappa$ for near-coplanar prograde and retrograde values (see green/dashed line in Figure 5). However, their $\epsilon$ values for HD 38529 (0.44), HD 168443 (0.219) and HD 190360 (0.38) are much less than the values of $\kappa$ for the near-planar regimes. Thus, we find that hierarchical systems typically have more moderate eccentricity evolution than suggested by Barnes & Greenberg (2006b). Hence, we do not find a significant discrepancy between the secular evolution of hierarchical two-planet systems and simulations of planet scattering. We find that the eccentricities of the inner planets in these systems vary by a factor of 2 or more for initial $i_{\rm rel,0}$ values closer to 90° than to 0° or 180°.

Libert & Henrard (2006) have studied the secular evolution of HD 38529 and HD 168443. The secular eccentricity evolution of the outer massive planet in HD 38529 is poorly modeled by low-order Laplace-Lagrange secular theory (Veras & Armitage 2007); N-body simulations in the coplanar, edge-on case indicate that the inner eccentricity evolves on a timescale of $\sim 10^5$ yr, and that the apsidal angle circulates. Libert & Henrard (2006) estimate that $\kappa_b = 0.87(0.90)$ and $\kappa_c = 0.999(0.999)$ for $i_{LOS} = 90°$ by using their high-order expansion (second-order Laplace-Lagrange theory in parenthesis). These values compare favorably with the values in the coplanar row of Table 4, with the difference attributed to our isotropic distribution of line-of-sight inclinations and choice of initial values for the orbital elements. We find slightly larger eccentricity evolution but qualitatively similar behavior. Libert & Henrard (2006) estimate that for $i_{LOS} = 90°$ and using their high-order expansion (Laplace-Lagrange theory), $\kappa_b = 0.85(0.89)$, and $\kappa_c = 0.83(0.91)$. The value of $\kappa_c$ differs significantly from our estimate (0.49) in Table 7. We believe this difference is due to the the increased masses resulting from our isotropic line-of-slight inclination distribution, resulting in a larger extent of eccentricity evolution of the outer planet.

Several researchers have considered the potential for additional small planets to exist in these systems, particularly those planets potentially in the habitable zone. Jones et al. (2006) considered likely habitable zone ranges, $h_z$ and habitability prospects (yes/no/maybe) for all 6 of the systems studied here. They found: HD 11964 ($h_z = 1.6 - 3.1$ AU, yes); HD 38529 ($h_z = 2.4 - 4.8$ AU, no); HD 108874 ($h_z = 1.0 - 2.0$ AU, no); HD 168443 ($h_z = 1.1 - 2.3$ AU, no); HD 12661 ($h_z = 1.0 - 2.0$ AU, no); HD 190360 ($h_z = 1.0 - 2.0$ AU, maybe). Érdi et al. (2004) agree that planets in the habitable zone of HD 38529 would likely have chaotic orbits. Similarly, both Érdi et al. (2004) and Barnes & Raymond (2004) agree that the prospects for stable planets in the habitable zone of HD 168443 are slim. Schwarz et al. (2007) raise the possibility that dynamically stable Trojan planets of HD 108874 b may exist in the habitable zone.

In order to help address the question of whether HD 190360 may admit habitable terrestrial planets, we perform 2 additional sets of 1 Myr simulations with a disk of test particles (a good representation of terrestrial planets in systems with giant planets). We start from the output of MCMC simulations and randomly chose 2 sets of stable coplanar initial orbital parameters for the system. For each system, we superimposed a coplanar disk of 40 terrestrial planets distributed in semimajor axis according to a Keplerian (power law of $-3/2$) distribution. We assigned the eccentricities of the planetesimals random values under 0.001 and randomized their mean anomalies and longitude of periastrons. The extent of the planetesimal disk was $[1.027, 2.022]$ AU (the same representative habitable zone values used by Jones et al. 2006) for one system, and $[0.128 \times (1 + 0.01), 3.92 \times (1 - 0.36)]$ AU (the representative range from the apocenter of the inner planet to the pericenter of the outer planet) for the other system. In the first (second) system, we find that 91.4% (92.7%) of all terrestrial planets survive within the initial planetesimal disk. The surviving planets have modest eccentricities: the median and standard deviation of these values are $0.18 \pm 0.12$ ($0.15 \pm 0.14$). Most initial instances of instability occur within $10^4$-$10^5$ yr. These results indicate that that HD 190360 can likely host a stable terrestrial planet in the habitable zone.

## 5. CONCLUSION

Due to limitations of real astronomical observations, often a significant range of planetary masses is consistent with observations. Therefore, it is necessary to investigate the dynamics of ensembles of planetary orbits and masses to accurately model the orbital evolution of exoplanets. Hierarchical multi-planet systems demonstrate a wide variety of dynamical behaviors depending on the $i_{LOS}$ and $i_{\rm rel}$ values, which are only weakly constrained by observations. Inclusion of GR in simulations of multi-planet systems with a Hot Jupiter may crucially affect the long-term stability, extent of eccentricity variation, and apsidal configuration directly. The eccentricity and inclination evolution of stable highly inclined systems are often dominated by Kozai-like oscillations, but can be limited by precession due to other planets or GR.

We thank the referee for helpful comments, Dan Fabrycky for assistance in characterizing the effect of general relativity, and Hal Levison and Jacques Laskar for useful discussions. We acknowledge the University of Florida High-Performance Computing Center for providing computational resources and support. This research was supported by NASA Origins of Solar Systems grant NNX09AB35G and JPL Research Support Agreement #1326409.

REFERENCES


Adams, F. C., & Laughlin, G. 2006, ApJ, 649, 992
Adams, F. C., & Laughlin, G. 2006, International Journal of Modern Physics D, 15, 2133
Anglada-Escude, G., Lopez-Morales, M., & Chambers, J. E. 2008, arXiv:0809.1275
Baluev, R. V. 2008, MNRAS, 389, 1375
Barnes, R., & Greenberg, R. 2006, ApJ, 638, 478
Barnes, R., & Greenberg, R. 2006, ApJ, 652, L53
Barnes, R., & Raymond, S. N. 2004, ApJ, 617, 569
Bean, J. L., & Seifahrt, A. 2009, arXiv:0901.3144
Beauge, C. 1994, Celestial Mechanics and Dynamical Astronomy, 60, 225
Beaugé, C. 1996, Celestial Mechanics and Dynamical Astronomy, 64, 313
Beaugé, C., Ferraz-Mello, S., & Michtchenko, T. A. 2003, ApJ, 593, 1124
Beaugé, C., & Michtchenko, T. A. 2003, MNRAS, 341, 760
Beaugé, C., Michtchenko, T. A., & Ferraz-Mello, S. 2006, MNRAS, 365, 1160
Beaugé, C., Giuppone, C. A., Ferraz-Mello, S., & Michtchenko, T. A. 2008, MNRAS, 385, 2151
Butler, R. P., et al. 2006, ApJ, 646, 505
Chambers, J. E. 1999, MNRAS, 304, 793
Chiang, E. I., & Murray, N. 2002, ApJ, 576, 473
Chiang, E. I., Tabachnik, S., & Tremaine, S. 2001, AJ, 122, 1607
Cincotta, P. M., & Simó, C. 2000, A&AS, 147, 205
Close, L. M., & Males, J. R. 2009, arXiv:0904.3936
Domingos, R. C., Winter, O. C., & Yokoyama, T. 2006, MNRAS, 373, 1227
Ellis, K. M., & Murray, C. D. 2000, Icarus, 147, 129
Érdi, B., Dvorak, R., Sándor, Z., Pilat-Lohinger, E., & Funk, B. 2004, MNRAS, 351, 1043
Fabrycky, D. C., & Murray-Clay, R. A. 2008, arXiv:0812.0011
Fabrycky, D., & Tremaine, S. 2007, ApJ, 669, 1298
Ferraz-Mello, S. 1994, Celestial Mechanics and Dynamical Astronomy, 58, 37
Ferraz-Mello, S., Beaugé, C., & Michtchenko, T. A. 2003, Celestial Mechanics and Dynamical Astronomy, 87, 99
Ferraz-Mello, S., Michtchenko, T. A., & Beaugé, C. 2005, ApJ, 621, 473
Fischer, D. A., Marcy, G. W., Butler, R. P., Vogt, S. S., Frink, S., & Apps, K. 2001, ApJ, 551, 1107
Fischer, D. A., et al. 2003, ApJ, 586, 1394
Fischer, D. A., et al. 2008, ApJ, 675, 790
Ford, E. B. 2005, AJ, 129, 1706
Ford, E. B. 2006, ApJ, 642, 505
Ford, E. B., Kozinsky, B., & Rasio, F. A. 2000, ApJ, 535, 385
Fukagawa, M., Itoh, Y., Tamura, M., Oasa, Y., Hayashi, S. S., Fujita, Y., Shibai, H., & Hayashi, M. 2009, ApJ, 696, L1
Gayon, J., Marzari, F., & Scholl, H. 2008, MNRAS, 389, L1
Gayon, J., & Bois, E. 2008, A&A, 482, 665
Gladman, B. 1993, Icarus, 106, 247
Goździewski, K. 2003, A&A, 398, 1151
Goździewski, K., Konacki, M., & Maciejewski, A. J. 2005, ApJ, 622, 1136
Goździewski, K., Konacki, M., & Maciejewski, A. J. 2006, ApJ, 645, 688
Goździewski, K., & Migaszewski, C. 2006, A&A, 449, 1219
Goździewski, K., & Migaszewski, C. 2009, MNRAS, L247
Gozdziewski, K., Migaszewski, C., & Musielinski, A. 2008, arXiv:0802.0254
Gregory, P. C. 2007, MNRAS, 374, 1321
Gregory, P. C. 2007, MNRAS, 381, 1607
Holman, M., Touma, J., & Tremaine, S. 1997, Nature, 386, 254
Jancart, S., Lemaitre, A., & Istace, A. 2002, Celestial Mechanics and Dynamical Astronomy, 84, 197
Ji, J., Liu, L., Kinoshita, H., Zhou, J., Nakai, H., & Li, G. 2003, ApJ, 591, L57
Ji, J.-H., Kinoshita, H., Liu, L., & Li, G.-Y. 2009, Research in Astronomy and Astrophysics, 9, 703
Jones, B. W., Sleep, P. N., & Underwood, D. R. 2006, ApJ, 649, 1010
Jordán, A., & Bakos, G. Á. 2008, ApJ, 685, 543
Kiseleva, L. G., Eggleton, P. P., & Mikkola, S. 1998, MNRAS, 300, 292
Kley, W., Lee, M. H., Murray, N., & Peale, S. J. 2005, A&A, 437, 727
Lafrenière, D., Marois, C., Doyon, R., & Barman, T. 2009, ApJ, 694, L148
Lee, M. H. 2004, ApJ, 611, 517
Lee, M. H., & Peale, S. J. 2003, ApJ, 592, 1201
Libert, A.-S., & Henrard, J. 2006, Icarus, 183, 186
Libert, A.-S., & Henrard, J. 2007, A&A, 461, 759
Libert, A.-S., & Henrard, J. 2008, Celestial Mechanics and Dynamical Astronomy, 100, 209
Libert, A.-S., & Tsiganis, K. 2009, A&A, 493, 677
Lin, D. N. C., Papaloizou, J. C. B., Terquem, C., Bryden, G., & Ida, S. 2000, Protostars and Planets IV, 1111
Marcy, G. W., et al. 2001, ApJ, 555, 418
Marois, C., Macintosh, B., Barman, T., Zuckerman, B., Song, I., Patience, J., Lafrenière, D., & Doyon, R. 2008, Science, 322, 1348
Mayor, M., Udry, S., Naef, D., Pepe, F., Queloz, D., Santos, N. C., & Burnet, M. 2004, A&A, 415, 391
Michtchenko, T. A., Beaugé, C., & Ferraz-Mello, S. 2006, Celestial Mechanics and Dynamical Astronomy, 94, 411
Michtchenko, T. A., Beaugé, C., & Ferraz-Mello, S. 2008, MNRAS, 387, 747
Michtchenko, T. A., Beaugé, C., & Ferraz-Mello, S. 2008, MNRAS, 391, 215
Michtchenko, T. A., Ferraz-Mello, S., & Beaugé, C. 2006, Icarus, 181, 555
Migaszewski, C., & Goździewski, K. 2009, MNRAS, 392, 2
Migaszewski, C., & Goździewski, K. 2009, MNRAS, 395, 1777
Michtchenko, T. A., & Malhotra, R. 2004, Icarus, 168, 237
Moorhead, A., & Ford, E.B. 2009, In Preparation
Morbidelli, A. 2002, Modern celestial mechanics : aspects of solar system dynamics, London: Taylor & Francis,
Moro-Martín, A., et al. 2007, ApJ, 658, 1312
Murray, C. D., & Dermott, S. F. 1999, Solar system dynamics by Murray, C. D., 1999,
Murray-Clay, R. A., & Chiang, E. I. 2005, ApJ, 619, 623
Namouni, F. 2005, AJ, 130, 280
Pireaux, S., & Rozelot, J.-P. 2003, Ap&SS, 284, 1159
Raymond, S. N., & Barnes, R. 2005, ApJ, 619, 549
Raymond, S. N., Barnes, R., & Gorelick, N. 2008a, ApJ, 689, 478
Raymond, S. N., Barnes, R., Armitage, P. J., & Gorelick, N. 2008b, ApJ, 687, L107
Raymond, S. N., Barnes, R., Veras, D., Armitage, P. J., Gorelick, N., & Greenberg, R. 2009, ApJ, 696, L98
Reidemeister, M., Krivov, A. V., Schmidt, T. O. B., Fiedler, S., Müller, S., Löhne, T., & Neuhäuser, R. 2009, arXiv:0905.4688
Sándor, Z., Kley, W., & Klagyivik, P. 2007, A&A, 472, 981
Schwarz, R., Dvorak, R., Pilat Lohinger, E., Süli, Á., & Érdi, B. 2007, A&A, 462,
Sidlichovský, M., & Nesvorný, D. 1994, A&A, 289, 972
Sudol, J. J., Assalita, S., Johnston, B., & Haghighipour, N. 2009, American Astronomical Society Meeting Abstracts, 214, #434.10
ter Braak, Cajo F. T. 2006, Stat Comput, 16, 239249.
Touma, J. R., Tremaine, S., & Kazandjian, M. V. 2009, MNRAS, 394, 1085
Udry, S., Mayor, M., Naef, D., Pepe, F., Queloz, D., Santos, N. C., & Burnet, M. 2002, A&A, 390, 267
Udry, S., Mayor, M., & Queloz, D. 2003, Scientific Frontiers in Research on Extrasolar Planets, 294, 17
Valtonen, M., & Karttunen, H. 2006, The Three-Body Problem, Cambridge University Press.
Veras, D. 2007, Celestial Mechanics and Dynamical Astronomy, 99, 197
Veras, D., & Armitage, P. J. 2004, Icarus, 172, 349
Veras, D., & Armitage, P. J. 2007, ApJ, 661, 1311
Veras, D., & Ford, E. B. 2009, ApJ, 690, L1
Vogt, S. S., Butler, R. P., Marcy, G. W., Fischer, D. A., Henry, G. W., Laughlin, G., Wright, J. T., & Johnson, J. A. 2005, ApJ, 632, 638
Vogt, S. S., Butler, R. P., Marcy, G. W., Fischer, D. A., Pourbaix, D., Apps, K., & Laughlin, G. 2002, ApJ, 568, 352
Voyatzis, G., & Hadjidemetriou, J. D. 2006, Celestial Mechanics and Dynamical Astronomy, 95, 259
Winter, O. C., & Murray, C. D. 1997, A&A, 328, 399
Wright, J. T., Upadhyay, S., Marcy, G. W., Fischer, D. A., Ford, E. B., & Johnson, J. A. 2008, arXiv:0812.1582
Zhou, J.-L., & Sun, Y.-S. 2003, ApJ, 598, 1290

## APPENDIX

Because most of our simulations treat planets with non-zero eccentricities, we derive a more general relation than that of Eq. (8). The two conserved quantities for a two-planet system including GR based on a quadrupole-order potential are[2]:

$$F = -\frac{z_1}{\sqrt{(1-e_{\rm inner}^2)}} + z_2 \left\{ -2 - 3e_{\rm inner}^2 + \left(3 + 12e_{\rm inner}^2 - 15e_{\rm inner}^2 \cos^2 \omega_{\rm inner}\right) \sin^2 I_{\rm rel,0} \right\}, \quad (1)$$

$$H^2 = z_3 \left(1 - e_{\rm inner}^2\right) \cos^2 I_{\rm rel,0}, \quad (2)$$

where

$$z_1 = \frac{3G^2 M_\star M_{\rm inner} \left(M_\star + M_{\rm inner}\right)}{a_{\rm inner}^2 c^2}, \quad (3)$$

$$z_2 = \frac{GM_\star M_{\rm inner} M_{\rm outer}}{M_\star + M_{\rm inner}} \frac{a_{\rm inner}^2}{8a_{\rm outer}^3 \left(1 - e_{\rm outer}^2\right)^{3/2}}, \quad (4)$$

$$z_3 = M_\star M_{\rm inner} \sqrt{\frac{G a_{\rm inner}}{M_\star + M_{\rm inner}}}. \quad (5)$$

Noting that $z_1/z_2 = 6P_{\rm Koz}\dot{\omega}_{\rm sec} = 12\pi/\chi_{\rm Kozai}$, one can then compute $F' \equiv F/z_2$ and $H'^2 \equiv H^2/z_3$ from the initial conditions and then solve the following implicit equation for $e_{\rm inner,max}$:

$$\cos^2 i_{\rm rel,0} = \frac{3}{5}\left(1 - e_{\rm inner,max}^2\right) - \frac{2}{5}\frac{1 - e_{\rm inner,max}^2}{e_{\rm inner,max}^2 - e_{\rm inner,0}^2}\left(\frac{1}{\sqrt{1-e_{\rm inner,0}^2}} - \frac{1}{\sqrt{1-e_{\rm inner,max}^2}}\right)\left(\frac{2\pi}{\chi_{\rm Kozai}}\right) \quad (6)$$

Because Eq. (6) may admit no solutions for certain values of $I_{\rm rel,0}$, one must consider the physically plausible solutions. When the inner planet's initial eccentricity equals zero, no Kozai librations occur for $\chi_{\rm Kozai} < 2\pi/3$. More generally, as a function of $e_{\rm inner,0}$, no Kozai librations occur when:

$$\chi_{\rm Kozai} < \frac{4\pi\left(1 - \sqrt{1-e_{\rm inner,0}^2}\right)}{3e_{\rm inner,0}^2\sqrt{1-e_{\rm inner,0}^2}}. \quad (7)$$

Equation (7) demonstrates that the critical $\chi_{\rm Kozai}$ for which Kozai oscillations will occur is a weak function of $e_{\rm inner,0}$ so that such oscillations should always occur for $\chi_{\rm Kozai} > 2\pi$ when $0 \leq e_{\rm inner,0} \lesssim 0.79$. The equations, however, are just approximations, because they assume 1) secular evolution only (no change in semimajor axis), 2) a Hamiltonian truncated to the quadruple-order term, 3) a doubly-averaged Hamiltonian which eliminates short-period terms, and 4) a fixed outer orbit whose orbital plane does not vary.

[2] Note that Eq. (17) of Fabrycky & Tremaine (2007) should read "$H'^2 = \left(1 - e_{\rm in}^2\right)\cos^2 i$."

TABLE 1
Ratio of Effects

| System Name | $\chi_{\rm sec}$ | $\chi_{\rm Kozai}$ | $\chi_{\rm tide}$ | $\chi_{\rm obl}$ |
|---|---|---|---|---|
| HD 11964 | 1.02 | 6.43 | 0.027 | 0.0036 |
| HD 38529 | 0.79 | 6.11 | 0.017 | 0.006 |
| HD 168443 | 94.4 | 628.7 | 0.0003 | 0.0013 |
| HD 190360 | 0.14 | 1.05 | 0.21 | 0.0022 |
| HD 108874 | 1869.7 | 11068.1 | 0.000003 | 0.00029 |

Note. — Values of the ratios, $\chi_{\rm sec} \equiv \dot{\omega}_{\rm sec}/\dot{\omega}_{\rm GR}$, $\chi_{\rm tide} \equiv \dot{\omega}_{\rm tide}/\dot{\omega}_{\rm GR}$ and $\chi_{\rm obl} \equiv \dot{\omega}_{\rm obl}/\dot{\omega}_{\rm GR}$. The table values indicate that general relativity may have an appreciable effect on the dynamical evolution of HD 11964, HD 38529 and HD 190360, and that in most cases for each of the 5 systems, effects from stellar oblateness and tidal effects are weak compared to those from general relativity. These values are computed from representative values of the minimum masses and orbital parameters of each system.

TABLE 2
HD 11964 WITHOUT GENERAL RELATIVITY

| $i_{\rm rel}$ | Stable | $e_{b,med}$ | $e_b$ curve | $\kappa_b$ | $e_{c,med}$ | $e_c$ curve | $\kappa_c$ | $i_{r,med}$ |
|---|---|---|---|---|---|---|---|---|
| $0°$ | 100.0% | 0.28 | $[0.028, 0.15, 0.30, 0.45, 0.57]$ | 0.92 | 0.068 | $[0.012, 0.055, 0.11, 0.17, 0.21]$ | 0.92 | $\cdots$ |
| $0° - 15°$ | 100.0% | 0.30 | $[0.032, 0.16, 0.32, 0.48, 0.61]$ | 0.90 | 0.069 | $[0.012, 0.055, 0.11, 0.17, 0.21]$ | 0.92 | $10.5°$ |
| $15° - 30°$ | 100.0% | 0.31 | $[0.035, 0.18, 0.35, 0.53, 0.67]$ | 0.75 | 0.071 | $[0.012, 0.052, 0.11, 0.16, 0.21]$ | 0.92 | $23.9°$ |
| $30° - 45°$ | 100.0% | 0.30 | $[0.035, 0.18, 0.36, 0.55, 0.69]$ | 0.47 | 0.074 | $[0.012, 0.052, 0.11, 0.16, 0.20]$ | 0.94 | $38.7°$ |
| $45° - 60°$ | 100.0% | 0.30 | $[0.045, 0.22, 0.44, 0.66, 0.83]$ | 0.32 | 0.068 | $[0.012, 0.052, 0.11, 0.16, 0.21]$ | 0.91 | $53.1°$ |
| $60° - 75°$ | 48.8% | 0.28 | $[0.045, 0.23, 0.47, 0.70, 0.89]$ | 0.24 | 0.074 | $[0.012, 0.052, 0.11, 0.16, 0.20]$ | 0.86 | $64.4°$ |
| $75° - 90°$ | 4.4% | 0.23 | $[0.048, 0.24, 0.48, 0.72, 0.92]$ | 0.17 | 0.038 | $[0.0083, 0.045, 0.092, 0.14, 0.18]$ | 0.57 | $83.7°$ |
| $90° - 105°$ | 4.6% | 0.30 | $[0.078, 0.27, 0.50, 0.74, 0.93]$ | 0.19 | 0.053 | $[0.0083, 0.038, 0.075, 0.12, 0.21]$ | 0.67 | $95.8°$ |
| $105° - 120°$ | 40.2% | 0.29 | $[0.045, 0.23, 0.46, 0.69, 0.87]$ | 0.25 | 0.067 | $[0.0083, 0.048, 0.098, 0.15, 0.24]$ | 0.87 | $116.6°$ |
| $120° - 135°$ | 99.6% | 0.30 | $[0.045, 0.23, 0.46, 0.69, 0.87]$ | 0.31 | 0.067 | $[0.012, 0.055, 0.108, 0.17, 0.21]$ | 0.90 | $127.1°$ |
| $135° - 150°$ | 100.0% | 0.30 | $[0.038, 0.20, 0.40, 0.59, 0.75]$ | 0.45 | 0.071 | $[0.012, 0.052, 0.11, 0.16, 0.21]$ | 0.93 | $141.9°$ |
| $150° - 165°$ | 100.0% | 0.29 | $[0.032, 0.17, 0.33, 0.49, 0.63]$ | 0.75 | 0.066 | $[0.0083, 0.045, 0.092, 0.14, 0.18]$ | 0.91 | $156.1°$ |
| $165° - 180°$ | 100.0% | 0.28 | $[0.035, 0.17, 0.35, 0.52, 0.66]$ | 0.89 | 0.076 | $[0.012, 0.055, 0.11, 0.16, 0.21]$ | 0.93 | $169.4°$ |

Note. — Summary of stability, eccentricity evolution, and relative inclination evolution for HD 11964 without the inclusion of GR arranged by bins of relative inclination (Column 1). Column 2 displays the percent of stable systems out of 500, Columns 3, 6 and 9 display median starting values, and Columns 4, and 7 display the 5, 25, 50, 75 and 95 percentiles of the time-averaged eccentricity across all stable integrations within the given initial relative inclinations. Columns 5 and 8 display the mean ratios of the minimum vs. maximum eccentricities obtained throughout the simulations.

TABLE 3
HD 11964 WITH GENERAL RELATIVITY

| $i_{\rm rel}$ | Stable | $e_{b,med}$ | $e_b$ curve | $\kappa_b$ | $e_{c,med}$ | $e_c$ curve | $\kappa_c$ | $i_{r,med}$ |
|---|---|---|---|---|---|---|---|---|
| $0°$ | 100.0% | 0.28 | $[0.028, 0.15, 0.30, 0.44, 0.57]$ | 0.95 | 0.068 | $[0.012, 0.052, 0.11, 0.16, 0.21]$ | 0.94 | $\cdots$ |
| $0° - 15°$ | 100.0% | 0.28 | $[0.028, 0.15, 0.30, 0.45, 0.57]$ | 0.93 | 0.068 | $[0.012, 0.052, 0.11, 0.16, 0.21]$ | 0.93 | $10.6°$ |
| $15° - 30°$ | 100.0% | 0.28 | $[0.028, 0.15, 0.30, 0.45, 0.57]$ | 0.83 | 0.068 | $[0.018, 0.098, 0.20, 0.29, 0.37]$ | 0.94 | $23.3°$ |
| $30° - 45°$ | 100.0% | 0.28 | $[0.035, 0.18, 0.36, 0.54, 0.69]$ | 0.61 | 0.068 | $[0.012, 0.055, 0.11, 0.16, 0.21]$ | 0.94 | $38.5°$ |
| $45° - 60°$ | 100.0% | 0.28 | $[0.042, 0.21, 0.41, 0.62, 0.79]$ | 0.36 | 0.068 | $[0.012, 0.055, 0.11, 0.16, 0.21]$ | 0.90 | $52.4°$ |
| $60° - 75°$ | 88.2% | 0.28 | $[0.045, 0.23, 0.46, 0.68, 0.87]$ | 0.27 | 0.066 | $[0.012, 0.052, 0.11, 0.16, 0.21]$ | 0.86 | $66.9°$ |
| $75° - 90°$ | 27.8% | 0.34 | $[0.048, 0.24, 0.48, 0.72, 0.92]$ | 0.28 | 0.064 | $[0.0083, 0.048, 0.098, 0.15, 0.21]$ | 0.83 | $81.8°$ |
| $90° - 105°$ | 23.6% | 0.33 | $[0.052, 0.24, 0.48, 0.72, 0.92]$ | 0.28 | 0.068 | $[0.0083, 0.048, 0.098, 0.15, 0.19]$ | 0.84 | $96.7°$ |
| $105° - 120°$ | 83.6% | 0.27 | $[0.045, 0.23, 0.45, 0.67, 0.85]$ | 0.26 | 0.068 | $[0.012, 0.055, 0.11, 0.16, 0.21]$ | 0.84 | $113.3°$ |
| $120° - 135°$ | 100.0% | 0.28 | $[0.042, 0.21, 0.41, 0.62, 0.78]$ | 0.34 | 0.068 | $[0.012, 0.055, 0.11, 0.17, 0.21]$ | 0.90 | $127.3°$ |
| $135° - 150°$ | 100.0% | 0.28 | $[0.042, 0.20, 0.41, 0.61, 0.77]$ | 0.59 | 0.068 | $[0.012, 0.052, 0.11, 0.16, 0.20]$ | 0.94 | $141.5°$ |
| $150° - 165°$ | 100.0% | 0.28 | $[0.038, 0.19, 0.38, 0.57, 0.73]$ | 0.83 | 0.068 | $[0.012, 0.058, 0.12, 0.18, 0.22]$ | 0.94 | $156.8°$ |
| $165° - 180°$ | 100.0% | 0.28 | $[0.028, 0.15, 0.30, 0.45, 0.57]$ | 0.93 | 0.068 | $[0.012, 0.052, 0.11, 0.16, 0.20]$ | 0.93 | $169.1°$ |

Note. — Same as Table 2 but incorporating the effects of GR.

TABLE 4
HD 38529 WITHOUT GENERAL RELATIVITY

Table 4 is located on www.dimitriveras.com

TABLE 5
HD 38529 WITH GENERAL RELATIVITY

Table 5 is located on www.dimitriveras.com

TABLE 6
HD 108874

Table 6 is located on www.dimitriveras.com

TABLE 7
HD 168443

Table 7 is located on www.dimitriveras.com

TABLE 8
HD 190360 WITHOUT GENERAL RELATIVITY

Table 8 is located on www.dimitriveras.com

TABLE 9
HD 190360 WITH GENERAL RELATIVITY

Table 9 is located on www.dimitriveras.com

TABLE 10
HD 11964 (WITH GENERAL RELATIVITY)

| $i_{\rm rel}$ | aligned | antialigned | other | RMS $\Delta\varpi'$ |
|---|---|---|---|---|
| $0°$ | 68.6% (68.4%) [59.8%] | 26.8% (30.8%) [6.2%] | 4.6% (0.8%) [34.0%] | $91.4° \pm 5.0°$ ($95.7° \pm 4.9°$) [$95.2° \pm 5.5°$] |
| $0° - 15°$ | 65.8% (66.8%) [60.6%] | 31.0% (32.4%) [8.8%] | 3.2% (0.8%) [30.6%] | $91.8° \pm 4.3°$ ($94.9° \pm 4.9°$) [$96.3° \pm 5.4°$] |
| $15° - 30°$ | 60.6% (66.2%) [54.4%] | 34.4% (32.6%) [10.2%] | 5.0% (1.2%) [35.4%] | $91.3° \pm 6.5°$ ($93.8° \pm 4.4°$) [$96.6° \pm 7.1°$] |
| $30° - 45°$ | 39.6% (57.0%) [41.2%] | 21.6% (39.0%) [13.2%] | 38.8% (4.0%) [45.6%] | $63.6° \pm 25.4°$ ($91.5° \pm 8.9°$) [$70.9° \pm 24.2°$] |
| $45° - 60°$ | 37.6% (51.2%) [19.0%] | 30.4% (30.4%) [6.6%] | 32.0% (18.4%) [74.4%] | $64.3° \pm 25.0°$ ($78.8° \pm 20.2°$) [$65.4° \pm 26.7°$] |
| $60° - 75°$ | 50.0% (54.2%) [15.6%] | 34.0% (35.4%) [9.0%] | 16.0% (10.4%) [75.4%] | $74.4° \pm 21.5°$ ($80.3° \pm 16.6°$) [$66.7° \pm 26.4°$] |
| $75° - 90°$ | 50.0% (54.7%) [36.4%] | 27.3% (41.7%) [13.6%] | 22.7% (3.6%) [50.0%] | $81.2° \pm 12.6°$ ($84.0° \pm 11.4°$) [$75.7° \pm 19.9°$] |
| $90° - 105°$ | 60.9% (40.7%) [13.0%] | 21.7% (55.9%) [21.7%] | 17.4% (3.4%) [65.2%] | $75.4° \pm 20.2°$ ($83.7° \pm 11.8°$) [$70.0° \pm 22.2°$] |
| $105° - 120°$ | 42.3% (40.0%) [17.3%] | 37.8% (47.4%) [8.4%] | 19.9% (12.7%) [74.3%] | $75.1° \pm 21.5°$ ($78.5° \pm 17.1°$) [$69.8° \pm 25.8°$] |
| $120° - 135°$ | 31.3% (35.0%) [19.2%] | 34.9% (44.6%) [8.0%] | 33.7% (20.4%) [72.7%] | $62.7° \pm 27.4°$ ($77.7° \pm 21.7°$) [$64.9° \pm 26.9°$] |
| $135° - 150°$ | 34.2% (55.0%) [34.0%] | 25.4% (39.8%) [15.2%] | 40.4% (5.2%) [50.8%] | $64.6° \pm 25.4°$ ($91.1° \pm 9.8°$) [$69.9° \pm 24.6°$] |
| $150° - 165°$ | 60.8% (61.4%) [48.6%] | 32.8% (36.6%) [12.6%] | 6.4% (2.0%) [38.8%] | $92.4° \pm 5.8°$ ($94.4° \pm 4.4°$) [$95.8° \pm 7.8°$] |
| $165° - 180°$ | 57.0% (78.8%) [52.0%] | 34.6% (20.6%) [11.2%] | 8.4% (0.6%) [36.8%] | $93.0° \pm 5.6°$ ($95.0° \pm 4.8°$) [$96.5° \pm 7.1°$] |

NOTE. — Summary of libration of $\Delta\varpi'$ about aligned configurations (Column 2), antialigned configurations (Column 3) and asymmetric configurations (Column 4) arranged by bins of relative inclination (Column 1) for HD 11964. Column 5 displays the root mean squared (RMS) libration and its standard deviation across different initial conditions about the most prevalent libration center. Values in parenthesis are computed when GR is included in the simulations, and values in square brackets refer to the libration of $\omega_{\rm in}$ measured with respect to the invariable plane.

TABLE 11
HD 38529 WITH GENERAL RELATIVITY

Table 11 is located on www.dimitriveras.com

TABLE 12
HD 108874

Table 12 is located on www.dimitriveras.com

TABLE 13
HD 168443

Table 13 is located on www.dimitriveras.com

TABLE 14
HD 190360

Table 14 is located on www.dimitriveras.com

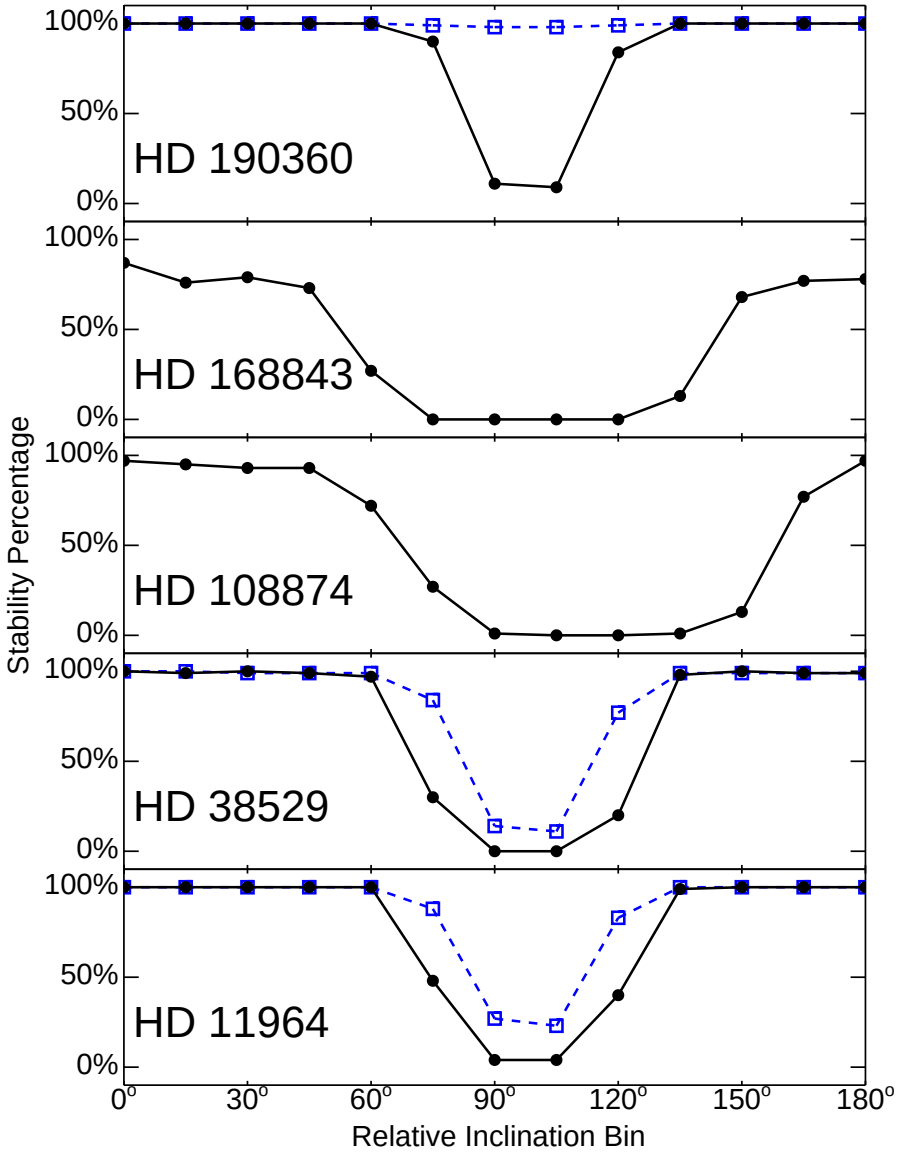


FIG. 1.— The percent of stable systems for HD 11964, HD 38529, HD 108874, HD 168443 and HD 190360 as a function of relative inclination when the effect of general relativity is included (blue/dashed lines and squares) and when it is not (black/solid lines and dots). The data points correspond to 15°-wide relative inclination bins along with a coplanar prograde bin.

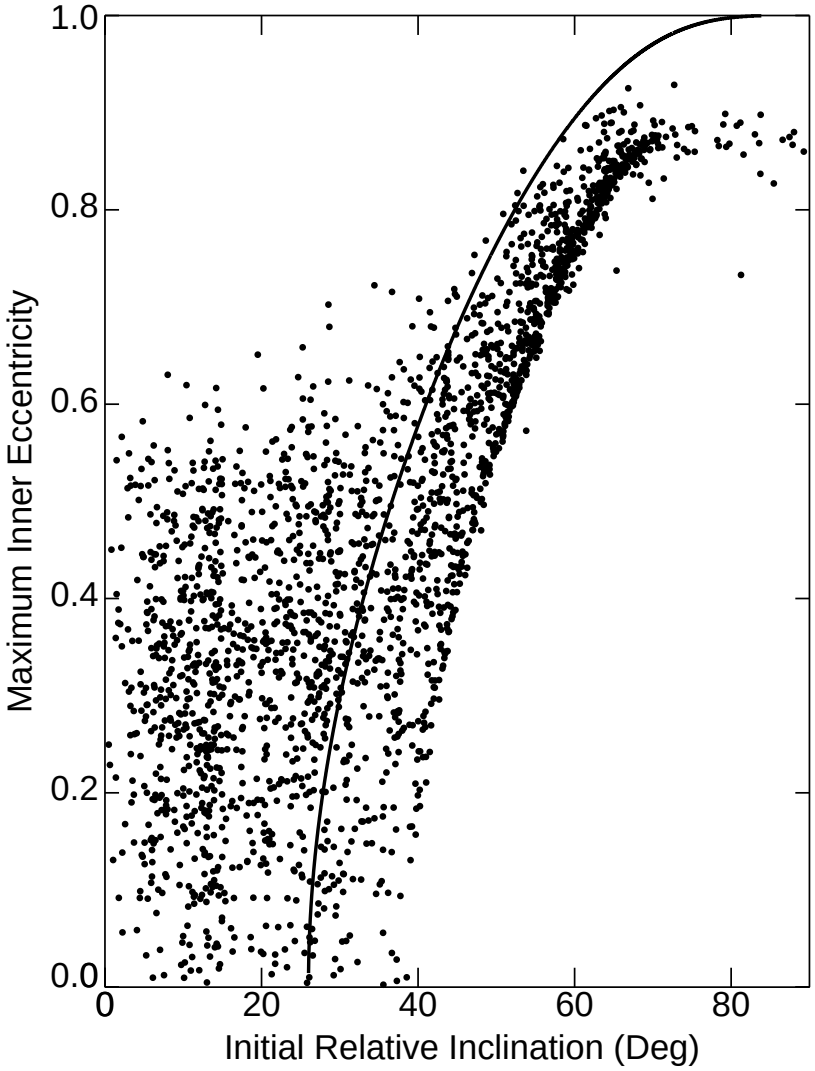


FIG. 2.— The maximum eccentricity achieved by the inner planet of HD 11964 for stable systems as a function of initial relative inclination (dots). Overlayed is the solid curve predicted from theory (Eq. 6) which predicts the maximum eccentricity attained by planets affected by general relativity, assuming an initial representative inner planet eccentricity of 0.28. Dots appear above the curve at low inclinations because in this regime, the eccentricity oscillations are not dominated by Kozai effects, but rather by classical Laplace-Lagrange secular theory.

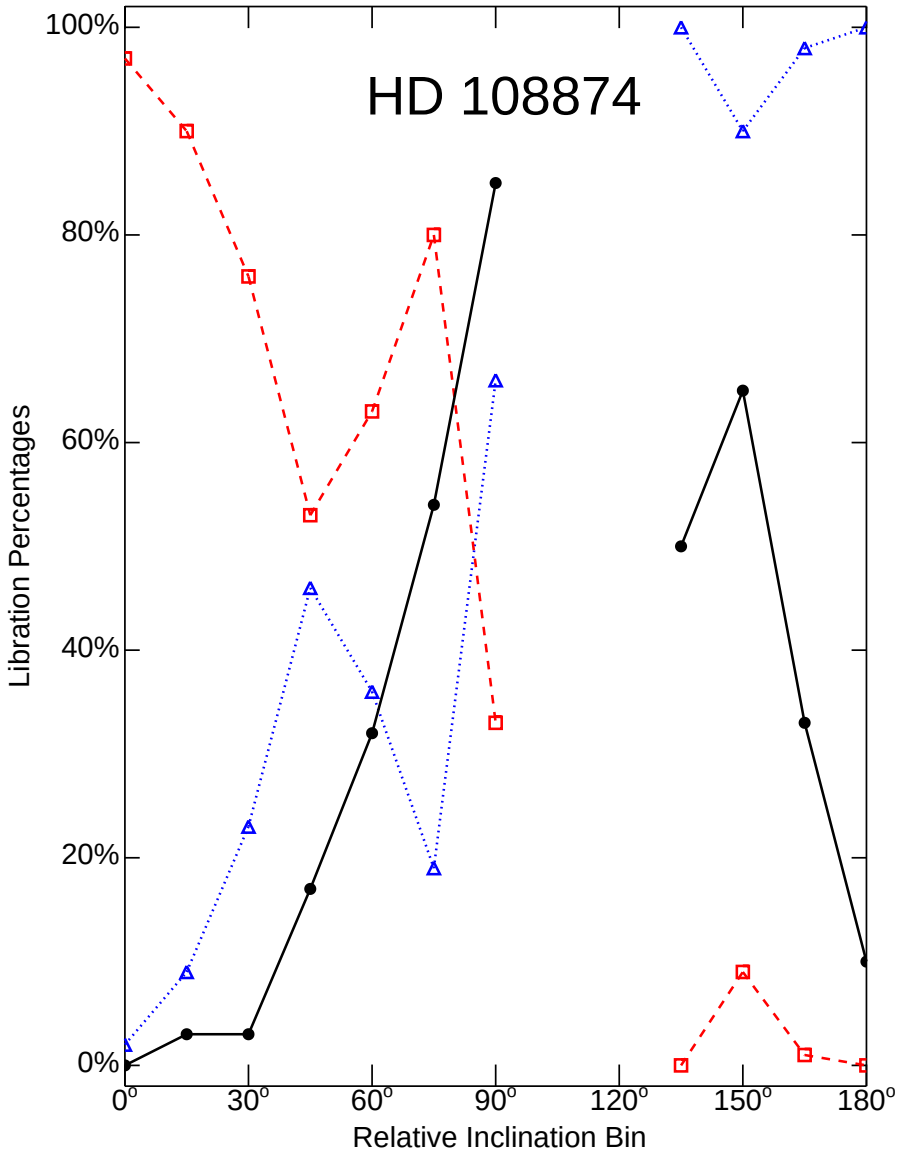


FIG. 3.— The percent of simulated HD 108874 stable systems whose apsidal angle projected on the invariable plane ($\Delta\varpi'$) is predominantly aligned (blue/dotted line with triangles) and antialigned (red/dashed line with squares). Overlayed is the percent of systems whose inner planet argument of pericenter measured with respect to the invariable plane librates around 90° or 270° in a Kozai-like fashion (black/solid line with dots). The data points correspond to 15°-wide relative inclination bins along with a coplanar prograde bin. Bins with no symbols or lines contain no stable systems.

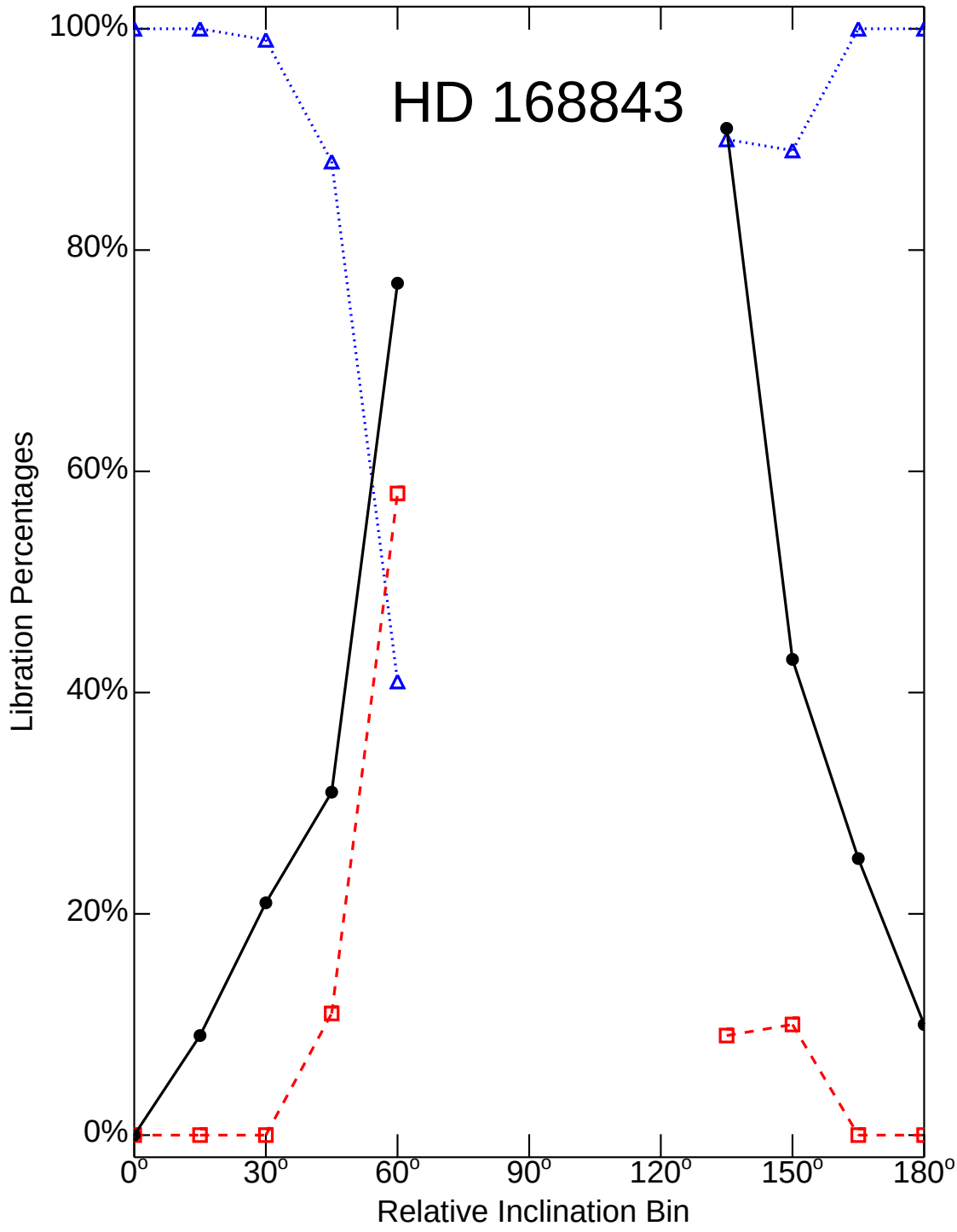


FIG. 4.— Same as Fig. 3 but for HD 168843, a system with two planets not near MMR.

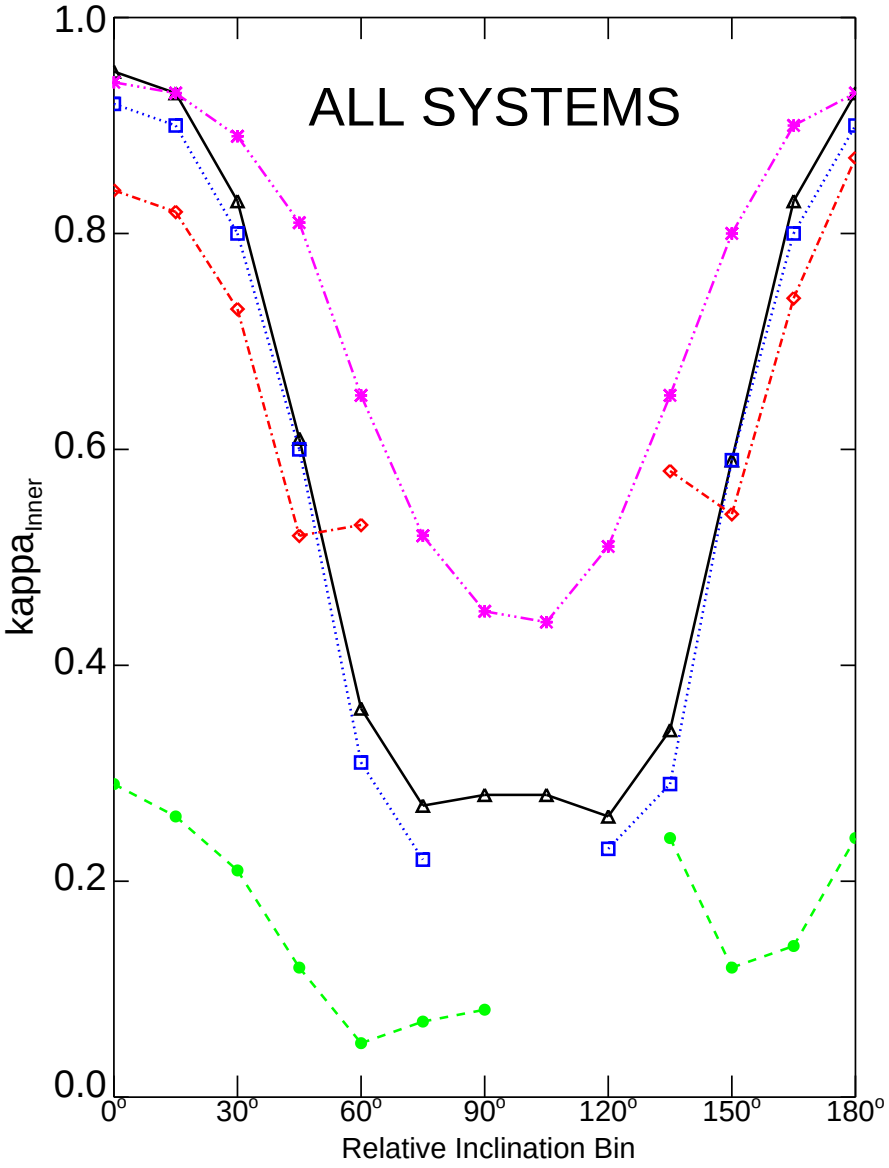


FIG. 5.— The averaged eccentricity variation ($\kappa \equiv e_{min}/e_{max}$) of the inner planet as a function of initial relative inclination for HD 11964 (black/solid lines with triangles), HD 38529 (blue/dotted lines with squares), HD 108874 (green/dashed lines with dots), HD 168443 (red/dot-dashed lines with diamonds) and HD 190360 (magenta/triple dot-dashed lines with asterisks). The data points correspond to 15°-wide relative inclination bins along with a coplanar prograde bin. Bins with no symbols or lines contain no stable systems.